Anisotropy of expandable graphite to explain its behavior as a flame-retardant

Tsilla Bensabath, Johan Sarazin, Serge Bourbigot

HAL Id: hal-03592692
https://hal.univ-lille.fr/hal-03592692v1

Anisotropy of expandable graphite to explain its behavior as a flame-retardant

Tsilla Bensabath[1], Johan Sarazin[1] and Serge Bourbigot[1,2]

Abstract

Expandable graphite is used as a flame-retardant in polymers. Its expansion on heating leads to a network of graphite worms which acts as a thermal barrier. However, mechanisms of action of worms are not yet well known. An original experimental approach is performed to study the heat dissipation in the network of worms. The network is made by the burning of polypropylene with 10 wt% expandable graphite during cone calorimeter experiment. After the burning, a hot spot is applied on the char. Temperature is monitored at different locations of sample during the combustion and after the application of the hot spot. During cone calorimetry, the char develops homogeneously over the whole sample. The hot spot test evidences the anisotropy of the entangled network of graphite worms. This anisotropy of heat conductivity allows the dissipation of heat in-plane and poorly out of plane, which explains the thermal barrier effect made by entangled worms.

Introduction

More and more plastics are used in many industrial sectors. However, organic polymer systems are highly flammable and they increase fire risks. That is why it is necessary to improve their fire behavior. A way to achieve this goal is the incorporation of fillers which act as flame-retardants (FRs) in the polymer matrix.[1]

[1]Univ. Lille, CNRS, INRAE, Centrale Lille, UMR 8207 - UMET - Unité Matériaux et Transformations, F-59000 Lille, France
[2]Institut Universitaire de France (IUF)

Corresponding author:
Serge Bourbigot, Univ. Lille, CNRS, INRAE, Centrale Lille, UMR 8207 - UMET - Unité Matériaux et Transformations, F-59000 Lille, France.
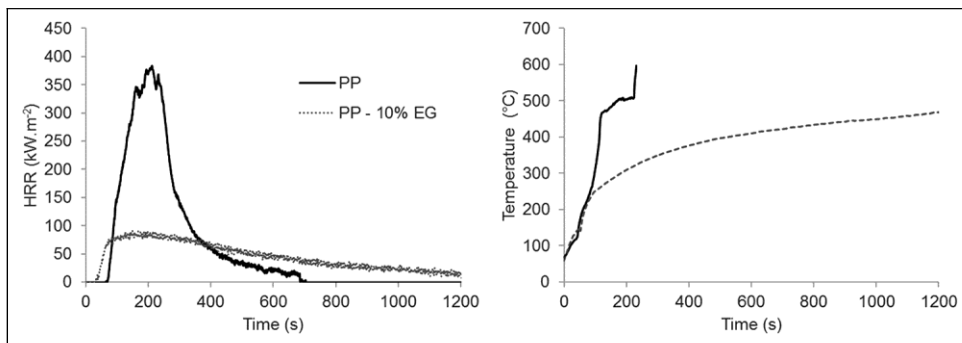Email: serge.bourbigot@univ-lille.fr

Figure 1. HRR (left) and temperature at the backside (right) as a function of time of neat PP and PP with 10 wt% EG during cone calorimeter experiments (external heat flux = 35 kW/m²).

Expandable graphite (EG) is used as an FR since the 2000s.[2,3] It is formed from natural mineral graphite, which is composed of superposed graphene layers. Compounds, such as acids (H_2SO_4, HNO_3, etc.), are intercalated between graphene layers and react with carbon atoms. EG can be synthesized by chemical or electrochemical processes.[3]

EG was first tested as an FR in polyethylene and polyurethane foams.[4] Afterward, many studies were carried out on different polymers. EG is used as the only FR in the polymer matrix[5–9] or in synergy with other FRs, such as modified ammonium polyphosphate (AP),[10–14] red phosphorus,[15,16] or aluminum tri-hydroxide.[17,18]

In a previous article, we studied the fire behavior of polypropylene (PP) blended with FRs: EG and AP, alone or combined in different ratios.[19] Samples of 100 ❸ 100 ❸ 3 mm³ were submitted to a heat flux of 35 kW/m² during a cone calorimeter experiment. In addition, a thermocouple was embedded at the backside of the 3-mm-thick samples to quantify the thermal barrier effect of FRs. Figure 1 presents heat release rate (HRR) curves and temperature profiles at the backside of samples obtained for neat PP and PP blended with 10 wt% EG. These graphs show that the addition of 10 wt% EG significantly improves the fire behavior of PP: peak of HRR (pHRR) and total heat release (THR) are decreased by 76% and 26% compared to neat PP, respectively. This blend also significantly improves the thermal barrier of PP.

The FR effect of EG is related to the physical phenomenon of expansion. When submitted to a heat source and from a specific temperature, intercalated compounds of EG quickly vaporize. They form gas pockets between graphene layers, which leads to a large expansion. When EG is used as an FR, flakes are generally mixed with the polymer. Their expansion leads to the formation of low-density elongated structures called graphite worms.[20,21] A non-cohesive char made of these worms is observed during the burning. It limits the transport of decomposition gases from the material and of oxygen from the flame and it acts as a thermal barrier protecting the polymer material from the action of the heat flux or the flame.[22]

However, these observations rise questions. As natural graphite, graphite worms obtained from the expansion of EG are known for their good heat conductivity[7] but they provide a thermal insulation effect. Moreover, in some cases, unexpected phenomena happen. In the previously quoted study,[19] when only 1 wt% EG is added in PP blended with 9 wt% AP, a fast temperature rise at the backside of sample is observed at the beginning of the burning

reaching high temperature before the temperature decreases and stabilizes. Graphite worms are trapped in a cohesive char due to AP and they increase the apparent thermal conductivity of intumescent PP. Therefore, the thermal barrier effect of EG depends on how the network of graphite worms is distributed and aligned.

Due to its layered structure, natural graphite is anisotropic. Its heat conductivity is different in-plane and out of plane: it is high within a graphene layer because of metallic bonds between carbon atoms but it is low perpendicular to layers because of weak Van der Waals forces between layers.[20] The aim of this article is to demonstrate, with a model case, that graphite worms also induce an anisotropy in the system, to better understand the mechanisms of action of EG when used as an FR. For this purpose, the dissipation of heat is studied through the network of worms obtained after the burning of a sample of PP blended with 10 wt% EG. An original experimental methodology is used to overcome the fact that the conductivity of graphite worms cannot be directly measured due to their structure.

Materials and methods

ES 350 F5 supplied by Graphitwerk Kropfmühl (Germany) was used as EG and blended with PP. This graphite has an expansion volume of 350 cm^3/g and it starts to expand around 200°C.

The mixture of 90 wt% PP and 10 wt% EG was prepared in a co-rotating intermeshing twin screw extruder. Plates of 100 ✗ 100 ✗ 6 mm^3 of FR polymer were made. These samples were submitted to an external heat flux of 35 kW/m^2 during a cone calorimeter test, until the total consumption of PP. Tests were carried out with a Fire Testing Technology (FTT) Mass Loss Calorimeter (MLC), following the procedure defined in ASTM E 906. A heat flux of 35 kW/m^2 was chosen because it corresponds to common heat flux in mild fire scenario[23,24] and because it allows a good development of graphite worms. All these steps of the experiment are detailed in a previous article.[19]

From the residue obtained after the cone calorimeter test, the study of heat conductivity of graphite worms was carried out following the procedure described below.

To be able to follow the temperature at different points of the residue, 28 thermocouples (K-type thermocouples of 0.5 mm diameter) were embedded vertically in the plates of PP–EG before the cone test, according to the scheme in Figure 2. Four sets of seven thermocouples were placed at different distances from the plate center (Figure 2(a)) and, for each set, thermocouples were placed at different heights (Figure 2(b)): at the backside of the plate (−6 mm), at the surface of the plate exposed to heat flux (0 mm), and at 5, 10, 15, 20 and 25 mm above the surface. These thermocouples also allowed to monitor temperatures in the plate and in the char during the cone calorimeter experiment.

After the combustion, the char constituted by graphite worms was around 34 mm high. Therefore, all thermocouples were into the material. This residue was cooled down. Then, a hot spot was applied at the top of the plate. It was performed with a calibrated flame by heating a metal part of 0.4 mm diameter inserted into a plate of calcium silicate placed 5 mm above the surface of the char. This device allows to gradually heat a specific point of the residue. The calcium silicate plate permits to create a thermal insulation and to avoid disturbances due to the flame and to the external environment on the surface of the residue. Moreover, the flame cannot be directly applied on the residue because of the risk of collapse of the non-cohesive structure. A thermocouple welded at the lowest point of the metal part
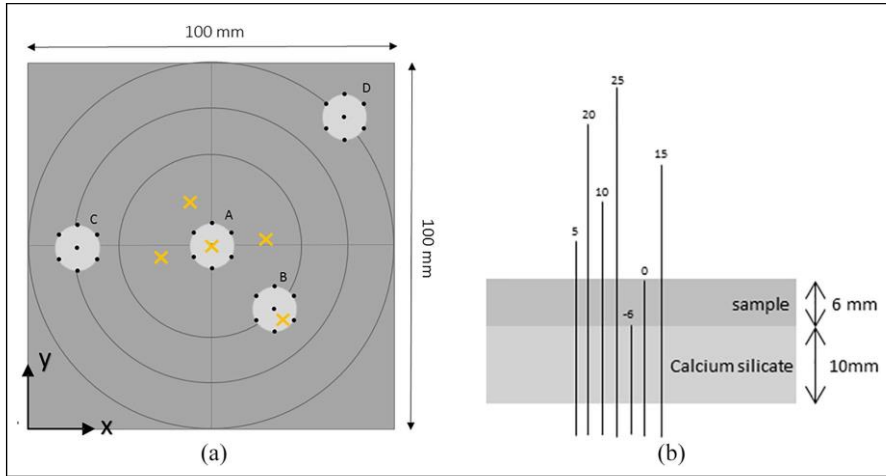
Figure 2. Disposition of thermocouples in samples of PP–EG: (a) horizontal disposition of the sets of thermocouples, (b) heights of thermocouples in each set in mm (0 mm represents the surface of the plate). Crosses on scheme a represent the locations of hot spots applied on the residue.
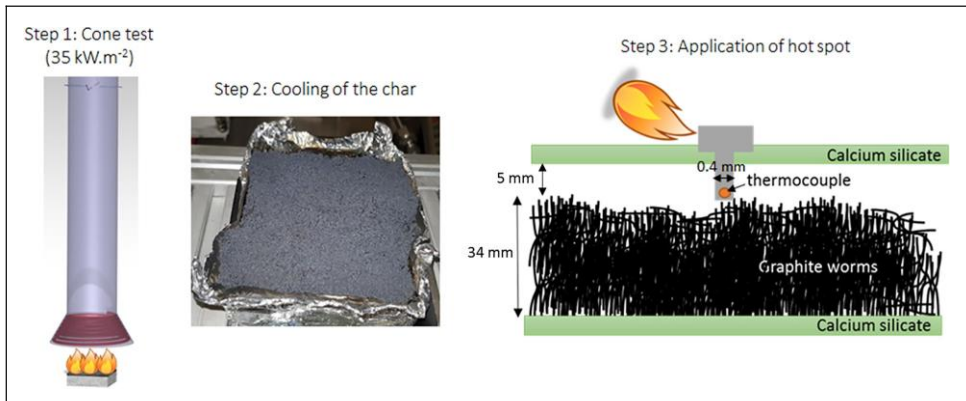

Figure 3. Procedure for the hot spot experiment.

gives the hot spot temperature throughout the experiment. This procedure is presented in Figure 3. Other thermocouples placed in the char allow to study the dissipation of heat by measuring the temperature at different distances from the hot spot, in both directions of space: vertically thanks to a same set of thermocouples (A, B, C, or D) and horizontally at a same height between the sets of thermocouples (see Figure 2).

The experiment was carried out on two samples, and different hot spots were successively applied at least at two places of the residue surface for each sample. The location of these different hot spots is showed on Figure 2(a) by crosses. This procedure allows to have more experimental points (more horizontal distances from the hot spot). It also allows to check
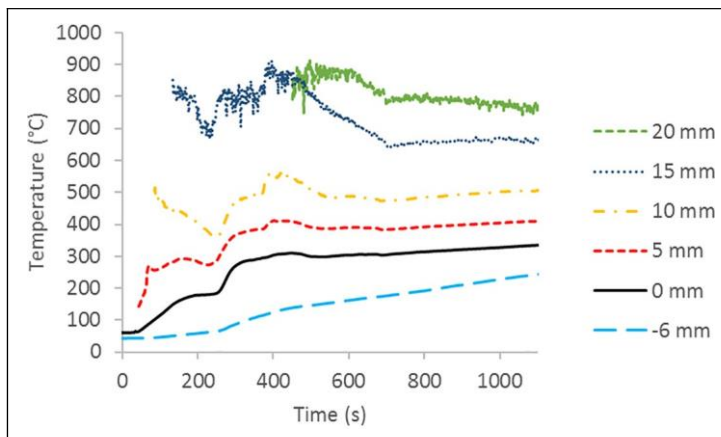
Figure 4. Temperature as a function of time at different heights in 6-mm-thick sample and in char of PP with 10 wt% EG during cone calorimeter experiment (external heat flux = 35 kW/m²)—0 mm is the height of the surface exposed to heat flux. Measurements are made in the center of the plate.

the repeatability of the experiment: at a same distance from the hot spot, the gap of temperature between two experiments is 20% maximum. The same maximal error of repeatability is observed for temperatures monitored during cone calorimeter tests. This gap can be explained by the uncertainty of 60.5 mm on the thermocouple placement. Temperature profile of the hot spot is also repeatable.

Results and discussion

Sample temperature during the graphite worm network formation

During the combustion with the cone calorimeter of the plate of PP blended with 10 wt% EG, embedded thermocouples were used to monitor temperature. Figure 4 presents the temperature profile of intumescent PP as a function of time and as a function of the distance to the surface of the plate (vertical profile). Results are those obtained in the center of the plate (set of thermocouples A in Figure 2(a)). Above the surface, temperature fluctuates during the phase of graphite expansion (thermocouples are covered by the char one by one) before stabilizing. The curve at 25 mm is not shown because the proximity of the cone resistance produces a phenomenon of incandescence, which disturbs the thermocouple measurements. At the backside of the sample (26 mm), temperature slowly increases. This last observation and the temperature gradient vertically obtained at the end of the experiment evidence the efficiency of the effect of thermal barrier generated by graphite worms.

Figure 4 presents results obtained at different heights in the center of the plate but a comparison of temperature profiles at different areas in the sample was also conducted for each height. As examples, Figure 5 presents this comparison at two heights: 26 mm (graph a), which is the backside of the sample and 20 mm (graph b), which corresponds to measurements in the char. In this last case, the char covers thermocouples from 450 s (vertical line in the graph of Figure 5(b)). Plots A, B, C, and D correspond to curves obtained in each area of thermocouples (see Figure 2(a)). At a given height, some gaps of temperature are
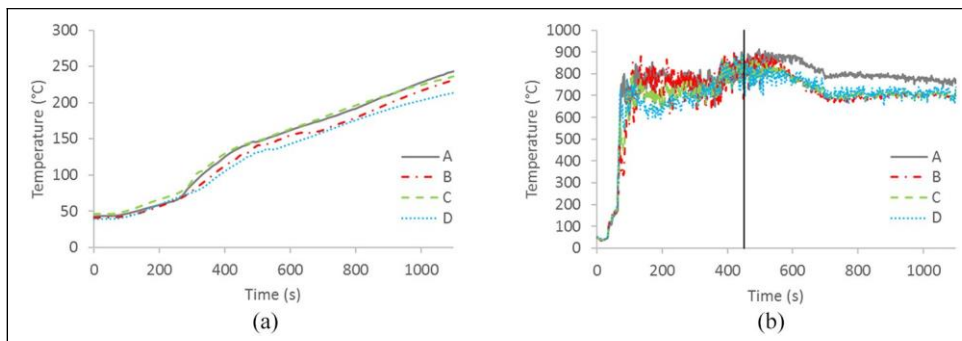
Figure 5. Comparison of temperature profiles in different places of the char (A, B, C, and D) at the same height of 26 mm (a: backside of the sample) and of 20 mm (b: 20 mm above the surface of the plate). Vertical line in (b) represents the time at which thermocouples are in the char.

sometimes observed between two points, particularly during the expansion phase for thermocouples above the surface (Figure 5(b)), but temperature changes are similar. Gaps can be explained by the non-homogeneity of heat flux (slightly higher in the center of the plate) and by the uncertainty on thermocouple height (60.5 mm). However, results show that the graphite worm network develops across the whole sample homogeneously. This is confirmed by visual observations during the experiment.

Heat dissipation in graphite worms

After cooling down the char residue, it was checked that the temperature was homogeneous at room temperature in the structure before applying the hot spot.

Arbitrarily, an experiment starts at time t_0, fixed when the hot spot reaches 150°C. From this time, temperatures at different locations in the char are monitored as a function of time and of hot spot temperature. A spatial origin is also fixed: point (0,0) is located 5 mm underneath the char surface, vertical to the hot spot. Heat dissipation is studied in the two directions of space from this point. Not taking the origin on the char surface avoids uncertainties related to the uneven surface.

Figure 6 presents the distribution of temperatures created by applying the hot spot in two ways. Graphs on the left are mapping of the char obtained from the measurements of thermocouples (indicated by crosses on graph a) and linearization between these measurements. They correspond to a vertical section of the plate made on the diagonal of the plane. Graphs on the right represent the horizontal and vertical temperature profiles from point (0,0). They come from the measurements of thermocouples. Parts a, b, and c of Figure 6 correspond to hot spot temperatures of 450°C, 560°C, and 580°C, respectively. These temperatures were chosen because they are approximately reached at $t_0 + 100$ s, $t_0 + 200$ s, and $t_0 + 300$ s, respectively. Parts d and e correspond to a hot spot temperature of 610°C, which is the temperature of stabilization. Part e was obtained 200 s after Part d.

Mapping allows to see a difference of heat propagation in the two directions of space. Graphs on the right quantify this difference. For any given temperature of the hot spot, at any given distance from point (0,0), the temperature measured horizontally is higher than
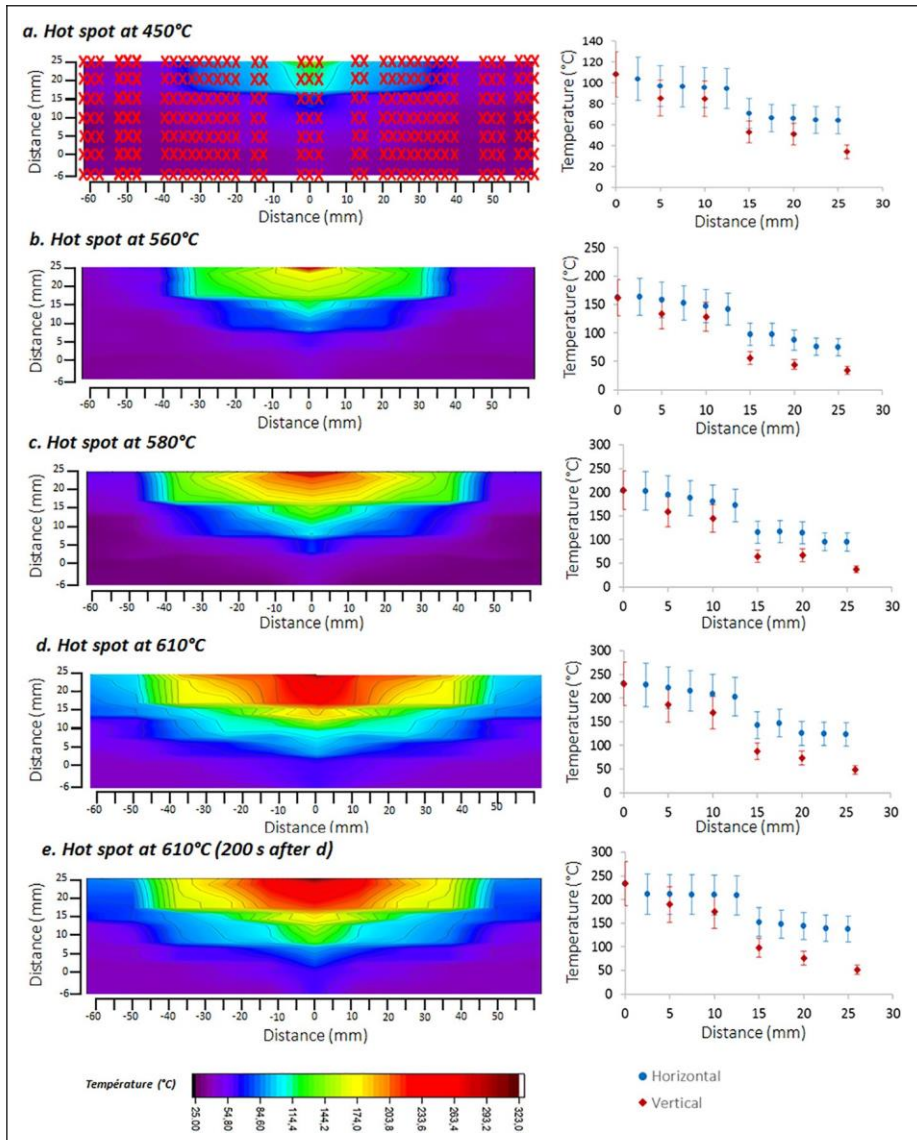
Figure 6. Mapping of temperatures (left) and comparison between vertical and horizontal temperatures as a function of the distance from the origin (right) in graphite worm network for several hot spot temperatures. Crosses on the first graph correspond to measurement locations (other points were obtained by linearization).

the temperature measured vertically. The decrease in temperature is faster in vertical direction. Heat conduction does not occur at the same velocity in the two directions of space and it gives evidence that the structure is anisotropic.

Figure 7 shows data of Figure 6 in a different way. The different plots represent the gap between horizontal and vertical temperatures at a same distance from the origin (DT) as a
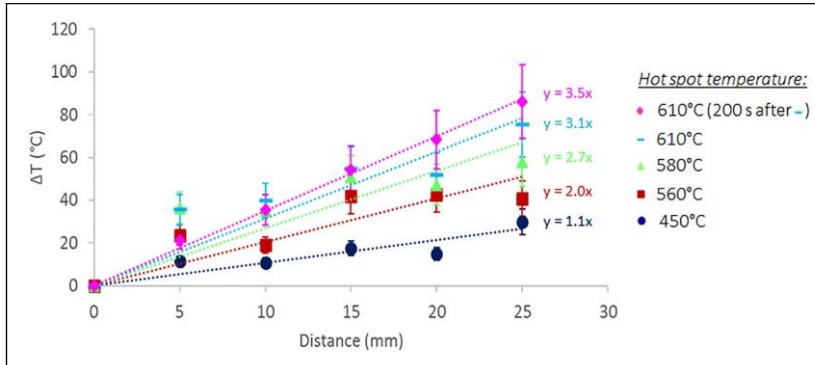
Figure 7. Gap between horizontal and vertical temperatures as a function of the distance from the origin for several hot spot temperatures.

function of this distance. Each plot corresponds to a temperature of the hot spot. This graph allows to better quantify the anisotropy because all data are on the same scale.

First, Figure 7 confirms that thermal conductivity is higher in horizontal than in vertical direction, even at low temperatures of the hot spot. Second, to compare the evolution as a function of hot spot temperature, each plot is linearized (in Figure 7, y is the slope). This linearization is not very representative because of the incertitude of measurements but it allows to highlight a general trend. It appears clearly that the gap between horizontal and vertical temperature increases with hot spot temperature. Then, it stabilizes when the temperature of the hot spot stabilizes. To have another point of view of this phenomenon, the ratio r between temperatures can be calculated as $r = \frac{T_{origin} - \delta T_{vertical} \flat_d}{T_{origin} - \delta T_{horizontal} \flat_d}$, with T_{origin} as the temperature at the origin, $(T_{vertical})_d$ and $(T_{horizontal})_d$ as the temperatures at a same distance d from the origin in vertical and in horizontal directions, respectively. As an example, for d = 20 mm, r varies from 1.35 to 1.76 for hot spot temperatures of 450°C and 610°C, respectively. It confirms the relative difference of heat propagation as a function of the direction and the increase in this difference with hot spot temperature.

These results allow to evidence a concept: the anisotropy for thermal conductivity of the network of graphite worms. A better understanding and quantification of this property could help to explain the good behavior of FR materials with graphite. The anisotropy of the char formed during the combustion induces a heat dissipation in-plane instead of through the material, which enhances the effect of thermal barrier of the material.

Conclusion

A study of heat dissipation through graphite worms was carried out. An entangled network of worms was obtained by the combustion of PP blended with 10 wt% EG during a cone calorimeter test. Temperature monitoring during the experiment shows that the char develops homogeneously over the whole sample. After cooling the char, a hot spot was applied and heat dissipation was analyzed thanks to several thermocouples embedded in the structure.

The results evidence the anisotropy of the entangled network of graphite worms. This property can explain the thermal insulation effect observed when EG is used as an FR in a polymer material while the graphite is known as a good heat conductor. Graphite worms allow the dissipation of heat in-plane. Therefore, the char acts as an efficient heat barrier.

To evidence the existence of the anisotropy phenomenon, some experimental conditions were chosen (for the formation of the char and for the application of the hot point). Afterward, it would be interesting to study the boundary conditions (especially temperature conditions) between which this phenomenon exists and how, in details, it can impact the fire properties of FR materials during different fire scenarios. To avoid experimental locks, a solution would be to use simulation to carry out this study.

Declaration of conflicting interests

Funding

References

1. Bourbigot S and Duquesne S. Fire retardant polymers: recent developments and opportunities. *J Mater Chem* 2007; 17: 2283–2300.
2. Xie R and Qu B. Expandable graphite systems for halogen-free flame-retarding of polyolefins. I. Flammability characterization and synergistic effect. *J Appl Polym Sci* 2001; 80: 1181–1189.
3. Duquesne S, Bras ML, Bourbigot S, et al. Analysis of fire gases released from polyurethane and fire-retarded polyurethane coatings. *J Fire Sci* 2000; 18: 456–482.
4. Focke WW, Badenhorst H, Mhike W, et al. Characterization of commercial expandable graphite fire retardants. *Thermochimica Acta* 2014; 584: 8–16.
5. Acuña P, Santiago-Calvo M, Villafañe F, et al. Impact of expandable graphite on flame retardancy and mechanical properties of rigid polyurethane foam. *Polym Compos* 2019; 40: E1705–E1715.
6. Sover A, Marzynkevitsch S and Munack B. Processing conditions of expandable graphite in PP and PA matrix and their performance. *Mater Plast* 2018; 55: 507–510.
7. Asante J, Modiba F and Mwakikunga B. Thermal measurements on polymeric epoxy-expandable graphite material. *Int J Polym Sci* 2016; 2016: 1–12.
8. Kruger HJ, Focke WW, Mhike W, et al. Thermal properties of polyethylene flame retarded with expandable graphite and intumescent fire retardant additives. *Fire Mater* 2017; 41: 573–586.
9. Bourbigot S, Sarazin J, Samyn F, et al. Intumescent ethylene-vinyl acetate copolymer: reaction to fire and mechanistic aspects. *Polym Degrad Stabil* 2019; 161: 235–244.
10. Bourbigot S, Sarazin J, Bensabath T, et al. Intumescent polypropylene: reaction to fire and mechanistic aspects. *Fire Safe J* 2019; 105: 261–269.
11. Awad WH and Wilkie CA. Investigation of the thermal degradation of polyurea: the effect of ammonium polyphosphate and expandable graphite. *Polymer* 2010; 51: 2277–2285.
12. Ge L-L, Duan H-J, Zhang X-G, et al. Synergistic effect of ammonium polyphosphate and expandable graphite on flame-retardant properties of acrylonitrile-butadiene-styrene. *J Appl Polym Sci* 2012; 126: 1337–1343.
13. Guo C, Zhou L and Lv J. Effects of expandable graphite and modified ammonium polyphosphate on the flame-retardant and mechanical properties of wood flour-polypropylene composites. *Polym Polym Compos* 2013; 21: 449–456.
14. Zhu H, Zhu Q, Li J, et al. Synergistic effect between expandable graphite and ammonium polyphosphate on flame retarded polylactide. *Polym Degrad Stabil* 2011; 96: 183–189.
15. Ji W, Yao Y, Guo J, et al. Toward an understanding of how red phosphorus and expandable graphite enhance the

fire resistance of expandable polystyrene foams. *J Appl Polym Sci* 2020; 1: 49045.

16. Modesti M and Lorenzetti A. Halogen-free flame retardants for polymeric foams. *Polymer Degrad Stabil* 2002; 78: 167–173.

17. Gunes OC, Gomek R, Tamar A, et al. Comparative study on flame retardancy, thermal, and mechanical properties of glass fiber reinforced polyester composites with ammonium polyphosphate, expandable graphite, and aluminum tri-hydroxide. *Arab J Sci Eng* 2018; 43: 6211–6218.

18. Wang W, He K, Dong Q, et al. Synergistic effect of aluminum hydroxide and expandable graphite on the flame retardancy of polyisocyanurate–polyurethane foams. *J Appl Polym Sci* 2014; 131: 39936.

19. Bensabath T, Sarazin J, Jimenez M, et al. Intumescent polypropylene: interactions between physical and chemical expansion. *Fire Mater* 2019; 1: 1–9.

20. Chung DDL. Review graphite. *J Mater Sci* 2002; 37: 1475–1489.

21. Duquesne S, Delobel R, Le Bras M, et al. A comparative study of the mechanism of action of ammonium polyphosphate and expandable graphite in polyurethane. *Polym Degrad Stabil* 2002; 77: 333–344.

22. Xie R and Qu B. Expandable graphite systems for halogen-free flame-retarding of polyolefins. II. Structures of intumescent char and flame-retardant mechanism. *J Appl Polym Sci* 2001; 80: 1190–1197.

23. Babrauskas V. Ignition sources. In: Babrauskas V (ed.) *Ignition handbook: principles and applications to fire safety engineering, fire investigation, risk management and forensic science*, 2003, pp. 497–590. Fire Science Publishers.

24. Schartel B and Hull T. Development of fire—retarded materials—interpretation of cone calorimeter data. *Fire Mater* 2007; 31: 327–354.